TITIPy: a Python tool for the calculation and mapping of Topside Ionosphere Turbulence Indices

Alessio Pignalberi

Istituto Nazionale di Geofisica e Vulcanologia, Via di Vigna Murata, 605, 00143, Rome, Italy

Abstract

TITIPy (*Topside Ionosphere Turbulence Indices with Python*) is a stand-alone Python tool developed for the calculation and mapping of RODI, ROTI, and ROTEI indices, for the characterization of the turbulent state of the topside ionosphere. Data gathered by Langmuir Probes and Precise Orbit Determination antennas on-board ESA Swarm satellites constellation are used to calculate topside ionosphere indices with a high time rate and a global coverage. From the study of these topside indices, information on physical mechanisms involved in the formation of small-scale irregularities (both spatial and temporal) can be drawn, particularly at high and low latitudes. TITIPy provides outputs as time series of calculated indices in text files, and figures as maps in geographic and magnetic coordinates. TITIPy is particularly suited for the investigation of the topside ionosphere irregularities, and for the identification of peculiar spatial and temporal patterns. The paper describes the TITIPy design and code workflow along with a detailed explanation of RODI, ROTI, and ROTEI indices calculation. Furthermore, an example of application based on data collected during the St. Patrick 2015 geomagnetic storm is also shown. TITIPy is open-source and freely downloadable at https://github.com/pignalberi/TITIPy.

Keywords: Topside ionosphere, RODI, ROTEI, ROTI, Python, ESA Swarm mission

Corresponding author: Alessio Pignalberi (alessio.pignalberi@ingv.it)

1. Introduction

The characterization of the physical state of the topside ionosphere is becoming more and more important in recent years due to the growing interest in the Space Weather applications (Moldwin, 2008). The topside ionosphere is the region extending from the F-layer peak (the ionospheric electron density maximum) to the *upper transition height* (Rishbeth and Garriott, 1969; Ratcliffe, 1972). A complete knowledge of the topside ionosphere is of topical importance for any satellite communication because it contains the largest fraction of the ionospheric total electron content (TEC); then, radio signals passing through it are affected by the presence of electrons that cause a change in the refraction index and then delays and phase shifts in signals. Moreover, it has also been recognized that small-scale fluctuations in the electron density can cause disrupting of communications between ground receivers and satellites (or between satellites), usually referred to as *loss of locks* (Buchert et al., 2015; Xiong et al. 2016). Despite its importance for Space Weather applications, the understanding of the topside ionosphere still remains a challenge because there are no continuous data available at the moment. In fact, topside electron density measurements are limited both in space and time by the difficulties in probing a region hidden to the widely spread ground-based ionosondes. As a consequence, more sophisticated and expensive techniques and instruments like incoherent scatter radars, topside sounders, radio-occultation, and in-situ Langmuir Probes on-board Low Earth Orbit (LEO) satellites, have to be employed to this task.

The topside ionosphere is very rich in electron density irregularities ranging from meters to hundreds of kilometers (Kelley, 2009). Electron density irregularities are customary at high latitudes (Tsunoda, 1988; Cherniak and Zakharenkova, 2016) and low latitudes (Zakharenkova and Astafyeva, 2015; Zakharenkova et

al., 2016); while middle latitudes are usually affected by them only under geomagnetic storms. To identify and study such irregularities in the topside electron density, two ionospheric indices were defined in the past: RODI (*Rate Of change of Density Index*) derived from in-situ electron density measurements, and ROTI (*Rate Of change of Total electron content Index*) derived from integrated TEC measurements. It has been shown that these indices can catch most of the irregularities and fluctuations exhibited by the topside electron density (Pi et al., 1997; Cherniak et al., 2014, 2015; Zakharenkova and Astafyeva, 2015; Cherniak and Zakharenkova, 2016; Zakharenkova et al., 2016; Jin et al., 2019; Piersanti et al., 2020). Recently, De Michelis et al. (2020), by analyzing electron density data from the ESA (*European Space Agency*) *Swarm* mission (Friis-Christensen et al., 2006) during a severe geomagnetic storm, were also able to associate RODI values and patterns (at high latitudes) to fluid and magnetohydrodynamic turbulence. Then, establishing a connection with the turbulent state of the upper atmosphere is topical.

ESA Swarm mission gives the opportunity to calculate topside ionosphere turbulence indices thanks to its three satellites orbit configuration and on-board instruments (Stolle et al., 2013). Langmuir Probes on-board Swarm satellites allow to calculate RODI values with a very high time rate and with a very good spatial coverage. At the same time, ROTI values can be obtained through *Precise Orbit Determination* (POD) antennas allowing to track *Global Positioning System* (GPS) satellites signals. This is why a *Python* (http://www.python.org/) tool has been developed aiming to calculate and map the ionospheric indices RODI and ROTI obtained through Swarm satellites data. The name of the tool is TITIPy (*Topside Ionosphere Turbulence Indices with Python*). Other than RODI and ROTI indices, TITIPy derives also a new index based on electron temperature measurements; its name is ROTEI (*Rate Of change of electron TEmperature Index*). For a specific time (year, month, and day defined by the user) and for a selected Swarm satellite (out of three), TITIPy automatically downloads needed files from the ESA Swarm repository, calculates ionospheric indices, and gives outputs as time series in text files and plots in geographic and magnetic coordinates. TITIPy is a stand-alone Python tool that does not require any installation apart from the required Python libraries and compilers; then, its use is very easy and straightforward. The use of TITIPy can help in the identification and investigation of topside ionosphere small-scale irregularities, thus highlighting their peculiar spatial and temporal patterns on a global scale. Its use is of particular interest in the study of the development and intensification of small-scale ionosphere irregularities under the specific and rapidly changing conditions imposed by geomagnetic storms. Moreover, TITIPy turns out to be suitable also for climatological studies to highlight the main features of small-scale ionosphere irregularities on a global scale and under different geophysical conditions (diurnal, seasonal, solar and magnetic activity variabilities).

In Section 2, ESA's Swarm mission and data are described. The definition and methodology applied for indices calculation is the topic of Section 3. Section 4 describes the TITIPy design and workflow, while an example of its application is given in Section 5. In Section 6, the conclusions are summarized.

2. ESA Swarm mission and data

Swarm is a ESA mission aiming to study the geomagnetic field, the impact of the solar wind on the dynamics of the upper atmosphere, and the electric currents in the magnetosphere and ionosphere (Friis-Christensen et al., 2006). Swarm is a constellation constituted by three LEO satellites launched at the end of 2013, and still operating, in a circular near-polar orbit. Two of them (Swarm A and C) have the same orbit configuration (inclination of 87.4°, initial altitude of about 460 km, east-west separation of about 1°–1.5° in longitude). The third (Swarm B) has a different orbital configuration (inclination of 88°, initial altitude of about 520 km) compared to the couple Swarm A and C. Swarm's data are freely downloadable at ftp://swarm-diss.eo.esa.int.

With regard to the design and instrumentation, the three Swarm satellites are identical. Among the instruments carried by Swarm satellites, we are here interested in Langmuir Probes (LP) (Knudsen et al., 2017) and POD antennas (van den Ijssel et al., 2016) data. LP provide measurements of in-situ electron density (*Ne*) and electron temperature (*Te*) with a 2-Hz rate (Swarm L1b Product Definition, 2018; Lomidze et al., 2018). Swarm Level 1b LP data (*EFIx_LP_1B*) contain time series of in-situ calibrated electron density and temperature data. No correction based on external instruments is applied to the Swarm Level 1b LP dataset.

Detailed information about Swarm data quality are available at https://earth.esa.int/web/guest/swarm/data-access/quality-of-swarm-l1b-l2cat2-products. POD antennas are GPS receivers from which the TEC is determined (Swarm L2 TEC Product Description, 2017; Noja et al., 2013). Level 2 TEC data (*TEC/TMS*) contain time series of vertical and slant (absolute and relative) TEC for each GPS satellite in view (at most eight due to instrumentation design). TEC time series are at 0.1 Hz until 15 July 2014, and at 1 Hz since than onwards.

Swarm's LP data are provided with three flags (Swarm L1b Product Definition, 2018); the first for LP instruments (*Flags_LP*), the other two characterizing electron density and temperature measurements (*Flags_Ne* and *Flags_Te*). For the calculation of indices derived from LP measurements, only the most reliable data are considered, namely those with *Flags_LP* = 1, *Flag_Ne* ≤ 29, and *Flags_Te* = 10 or 20. Differently, no flag is provided with TEC data; then, all data TEC are used for the indices calculation.

3. Topside ionosphere turbulence indices

By means of *N*e, *T*e, and TEC measured time series, it is possible to calculate some indices characterizing their fluctuations at small spatial and temporal scales in the topside ionosphere. These fluctuations are characteristic of phenomena happening in the topside ionosphere due mostly to the forcing imposed by the geomagnetic field configuration, solar illumination, neutral atmosphere dynamics, and coupling with the magnetosphere and solar wind (Rishbeth and Garriott, 1969; Ratcliffe, 1972; Tsunoda, 1988; Kelley, 2009). Swarm satellites data have recently allowed the identification of connections between turbulence phenomena and these ionospheric indices at high latitudes (Jin et al., 2019; De Michelis et al., 2020), and low latitudes (Zakharenkova et al., 2016; Xiong et al., 2016), in the topside ionosphere.

Swarm satellites derived data are particularly suited for ionospheric indices calculation and study due to their high measurement rate instrumentation and orbit configuration (as described in Section 2). The mathematical steps behind the topside ionosphere turbulence indices calculation are the same when considering *N*e, *T*e, and TEC measured time series. The indices calculation procedure is based on the following three mathematical steps:

1. From the measured time series of either *N*e, *T*e, or TEC, the corresponding time derivative along the satellite's orbit, at time *t*, is calculated:

$$\frac{\partial x(t)}{\partial t} = \frac{x(t+\delta t) - x(t)}{\delta t}, \tag{1}$$

   where *x* stands for either *N*e, *T*e, or TEC time series, and δt is the time step;

2. Time derivative calculated values are organized in sliding windows of width Δt centered at time *t*. In each window, the arithmetic mean of time derivative values is calculated by using all values falling between (t - $\Delta t/2$) and (t + $\Delta t/2$):

$$\overline{\frac{\partial x(t)}{\partial t}} = \frac{1}{N} \sum_{t_i = t-\Delta t/2}^{t+\Delta t/2} \frac{\partial x(t_i)}{\partial t}, \tag{2}$$

   Where *N* is the number of values falling in the window, depending on the window's width and time step;

3. The standard deviation of time derivative calculated values in a sliding window represents the index *X* associated to the physical quantity *x*:

$$X(t) = \sqrt{\frac{1}{N-1} \sum_{t_i = t-\Delta t/2}^{t+\Delta t/2} \left| \frac{\partial x(t_i)}{\partial t} - \overline{\frac{\partial x(t)}{\partial t}} \right|^2}. \tag{3}$$

Steps 1-3 are repeated along the entire time series of data measured by Swarms satellites to obtain time series of calculated indices.

3.1 Electron density and RODI

From electron density measurements the index named *Rate Of change of Density Index* (RODI, Zakharenkova and Astafyeva, 2015; Zakharenkova et al., 2016; Jin et al., 2019; De Michelis et al., 2020; Piersanti et al., 2020) can be derived by applying steps 1-3 to Swarms' measured data.

Specifically, the *Rate Of change of Density* (ROD) is the time derivative of the electron density calculated along the satellite's orbit. *N*e values measured by LP on-board Swarm satellites are continuous time series; however, missing measurements are possible. By indexing with k the contiguous measured values, the k^{th} ROD value is defined as:

$$\mathrm{ROD}_k = \frac{Ne_{k+1} - Ne_k}{t_{k+1} - t_k}\,, \tag{4}$$

where Ne_k is the electron density measured at time t_k. ROD values are calculated only for time consecutive measurements; i.e., when the condition $(t_{k+1} - t_k) = \delta t = 0.5$ s is met. As stated in (4) (the same applies in (7) and (10)), only the first-order term is considered in the calculation of the time derivative, i.e., only time consecutive values are considered. More refined numerical approaches based on higher-order terms might be applied at the cost of increasing the computational time. In TITIPy, the simplest first-order approach is applied to be consistent with the published literature on the topic, and to keep low the computational time.

Then, by application of (2) and (3), the k^{th} RODI value is calculated as:

$$\mathrm{RODI}_k = \sqrt{\frac{1}{N-1}\sum_{i=-j}^{j}\left|\mathrm{ROD}_{k+i} - \overline{\mathrm{ROD}}_k\right|^2}\,, \tag{5}$$

where ROD_{k+i} are ROD values falling inside the rectangular window centered at the index k, and of width $(2j + 1)$. The width of the window used for indices calculation is crucial for the detection of fluctuations of different spatial and temporal scales. For example, concerning the study of small-scale fluctuations, a good choice is to select windows 10-seconds wide as was done by De Michelis et al. (2020). This is also the default in TITIPy; then, $j = 10$ and (at most) 21 values are used for the RODI calculation (because of LP 2Hz rate). However, the user can change the width of the window used for indices calculation. In (5), $\overline{\mathrm{ROD}}_k$ is calculated by applying (2) to (4):

$$\overline{\mathrm{ROD}}_k = \frac{1}{N}\sum_{i=-j}^{j}\mathrm{ROD}_{k+i}\,. \tag{6}$$

RODI is calculated only when at least half of the values allowed in the window are present; otherwise, it is considered non statistically significant and then discarded. Then, in the default case where $\Delta t = 10$ s and $\delta t = 0.5$ s, at least 11 ROD values falling in the window are needed for the RODI calculation.

3.2 Electron temperature and ROTEI

The same procedure of Section 3.1, applied on electron density values to calculate RODI, has been applied on electron temperature values to obtain the index named *Rate Of change of electron TEmperature Index* (ROTEI). ROTEI is a new index which is presented here for the first time. ROTEI describes the small spatial and temporal scale fluctuations in the electron temperature along the Swarm satellites orbit. As a consequence, its use can be important to identify steep gradients in the topside ionosphere, associated for example with plasma heating caused by particle precipitation at auroral latitudes, or particles acceleration due to magnetic and electric fields.

The *Rate Of change of electron TEmperature* (ROTE) is the time derivative of the electron temperature calculated along the satellite's orbit:

$$\mathrm{ROTE}_k = \frac{Te_{k+1} - Te_k}{t_{k+1} - t_k} . \tag{7}$$

By application of (2) and (3), the k^{th} ROTEI value is calculated as:

$$\mathrm{ROTEI}_k = \sqrt{\frac{1}{N-1}\sum_{i=-j}^{j}\left|\mathrm{ROTE}_{k+i} - \overline{\mathrm{ROTE}}_k\right|^2} , \tag{8}$$

with

$$\overline{\mathrm{ROTE}}_k = \frac{1}{N}\sum_{i=-j}^{j}\mathrm{ROTE}_{k+i} . \tag{9}$$

3.3 Total electron content and ROTI

From TEC measurements the index named *Rate Of change of Total electron content Index* (ROTI, Pi et al., 1997; Cherniak et al., 2014, 2015; Cherniak and Zakharenkova, 2016) can be derived by applying steps 1-3 to Swarm TEC retrieved data. However, the application of mathematical steps 1-3 to TEC values requires special care because of two main reasons:

- Unlike *N*e and *T*e, TEC values are not in-situ measurements but integrated ones along the path linking the LEO Swarm satellite to the GPS satellite. In fact, TEC represents the total electron content obtained by integration of electron density between the Swarm and the GPS satellites positions. How slant and vertical TEC values are obtained through Swarm data is described in Swarm L2 TEC Product Description (2017). This means that measured TEC values (regardless of slant or vertical) cannot be associated to the Swarm orbit position;
- While a single value of *N*e and *T*e is available at a specific time, Swarm satellites can track at most eight GPS satellites simultaneously. This means that, for a specific time, we have to handle more TEC measurements coming from different GPS satellites, then from different locations.

How TITIPY faces these two issues is described in the following.

The *Rate Of change of Total electron content* (ROT) is the time derivative of the TEC calculated along the path linking Swarm to a specific GPS satellite. For the sake of simplicity, in the following, we simply refer to TEC values, taking in mind that both slant (sTEC) and vertical (vTEC) values can be used in the ROT derivation. Then:

$$\mathrm{ROT}_k^s = \frac{\mathrm{TEC}_{k+1}^s - \mathrm{TEC}_k^s}{t_{k+1} - t_k} , \tag{10}$$

where *s* is the index running on the GPS satellites in view. GPS satellites are identified by a Pseudo-Random Number (PRN), with PRN running from 1 to 32.

By application of (2) and (3), the k^{th} ROTI value, for the GPS satellite *s*, is calculated as:

$$\mathrm{ROTI}_k^s = \sqrt{\frac{1}{N-1}\sum_{i=-j}^{j}\left|\mathrm{ROT}_{k+i}^s - \overline{\mathrm{ROT}_k^s}\right|^2} , \tag{11}$$

with

203 $$\overline{\mathrm{ROT}_k^s} = \frac{1}{N}\sum_{i=-j}^{j} \mathrm{ROT}_{k+i}^s \,. \tag{12}$$

204 Level 2 TEC data (*TEC/TMS*) contain time series of vertical and slant (absolute and relative) TEC for each
205 GPS satellite in view (Swarm L2 TEC Product Description, 2017), along with Swarm and GPS satellites
206 coordinates in the Cartesian system of reference identified by the World Geodetic System 84 (WGS 84). WGS
207 84 is an Earth-centered Earth-fixed right-handed Cartesian coordinate system describing the Earth surface as
208 an oblate spheroid with equatorial radius 6378137.0 m and flattening 1/298.257223563 (Leick et al., 2015; Xu
209 and Xu, 2015). From here on, we will refer to this as *Global Cartesian coordinate system*, being centered on
210 the Earth's center of mass. However, due to the fact that Swarm satellites are orbiting the Earth, the most
211 suitable coordinate system is that centered on the Swarm satellite, that we will refer to as *Local Cartesian*
212 *coordinate system*. In the Local coordinate system, the *x* axis points to the North, the *z* axis along the local
213 vertical (i.e., the normal to the ellipsoidal surface identified by WGS 84), and the *y* axis is oriented to the right
214 of *x*. The Global and Local coordinate systems are depicted in panel a) of Figure 1. In the Global coordinate
215 system, the coordinates of the GPS satellite are $(x_{\mathrm{GPS}}, y_{\mathrm{GPS}}, z_{\mathrm{GPS}})$, while those for Swarm
216 $(x_{\mathrm{SWARM}}, y_{\mathrm{SWARM}}, z_{\mathrm{SWARM}})$. By following Xu and Xu (2015), the coordinates vector linking the GPS to the
217 Swarm satellite $(x_{\mathrm{GPS}} - x_{\mathrm{SWARM}}, y_{\mathrm{GPS}} - y_{\mathrm{SWARM}}, z_{\mathrm{GPS}} - z_{\mathrm{SWARM}})$ can be transformed from the Global to the Local
218 coordinate system. By defining $\mathbf{X_{Local}}$ as the vector of coordinates in the Local system, and $\mathbf{X_{Global}}$ as the
219 corresponding vector in the Global system, the two vectors are linked through the rotation matrix **R** defined in
220 (13).

221 $$\begin{cases} \mathbf{X_{Local}} = \mathbf{R}\mathbf{X_{Global}} \\ \mathbf{R} = \begin{pmatrix} -\sin\varphi\cos\lambda & -\sin\varphi\sin\lambda & \cos\varphi \\ -\sin\lambda & \cos\lambda & 0 \\ \cos\varphi\cos\lambda & \cos\varphi\sin\lambda & \sin\varphi \end{pmatrix} \end{cases}, \tag{13}$$

222 where φ is the geodetic latitude and λ the geodetic longitude of Swarm satellite (Figure 1); i.e., the origin of
223 the Local coordinate system. The matrix **R** is obtained by two successive rotations of the Global coordinate
224 system (a rotation of angle 90°- φ around the y_{Global} axis, followed by a rotation of angle λ around the z_{Global}
225 axis) and then by changing the x_{Local} axis to a right-handed system (Xu and Xu, 2015).

226 Eqs. (13) are then applied to our specific case comprising Swarm and GPS satellites:

227 $$\begin{cases} x'_{\mathrm{GPS}} = -(x_{\mathrm{GPS}} - x_{\mathrm{SWARM}})\sin\varphi\cos\lambda - (y_{\mathrm{GPS}} - y_{\mathrm{SWARM}})\sin\varphi\sin\lambda + (z_{\mathrm{GPS}} - z_{\mathrm{SWARM}})\cos\varphi \\ y'_{\mathrm{GPS}} = -(x_{\mathrm{GPS}} - x_{\mathrm{SWARM}})\sin\lambda + (y_{\mathrm{GPS}} - y_{\mathrm{SWARM}})\cos\lambda \\ z'_{\mathrm{GPS}} = (x_{\mathrm{GPS}} - x_{\mathrm{SWARM}})\cos\varphi\cos\lambda + (y_{\mathrm{GPS}} - y_{\mathrm{SWARM}})\cos\varphi\sin\lambda + (z_{\mathrm{GPS}} - z_{\mathrm{SWARM}})\sin\varphi \end{cases}, \tag{14}$$

228 where $(x'_{GPS}, y'_{GPS}, z'_{GPS})$ are the GPS coordinates in the Local coordinate system centered on the Swarm
229 satellite position.

230 Finally, the Azimuth (*Az*), Zenith (*Ze*), and Elevation (*El*) angles, in the Local coordinate system, can be
231 deduced by simple trigonometric relations (see panel a) of Figure 1):

$$\begin{cases} Ze = \arccos\left(\dfrac{z'_{\mathrm{GPS}}}{d}\right) \\ Az = \arctan\left(\dfrac{y'_{\mathrm{GPS}}}{x'_{\mathrm{GPS}}}\right), \\ El = \dfrac{\pi}{2} - Ze \end{cases} \tag{15}$$

where $d = \sqrt{\left(x_{\mathrm{GPS}} - x_{\mathrm{SWARM}}\right)^2 + \left(y_{\mathrm{GPS}} - y_{\mathrm{SWARM}}\right)^2 + \left(z_{\mathrm{GPS}} - z_{\mathrm{SWARM}}\right)^2}$.

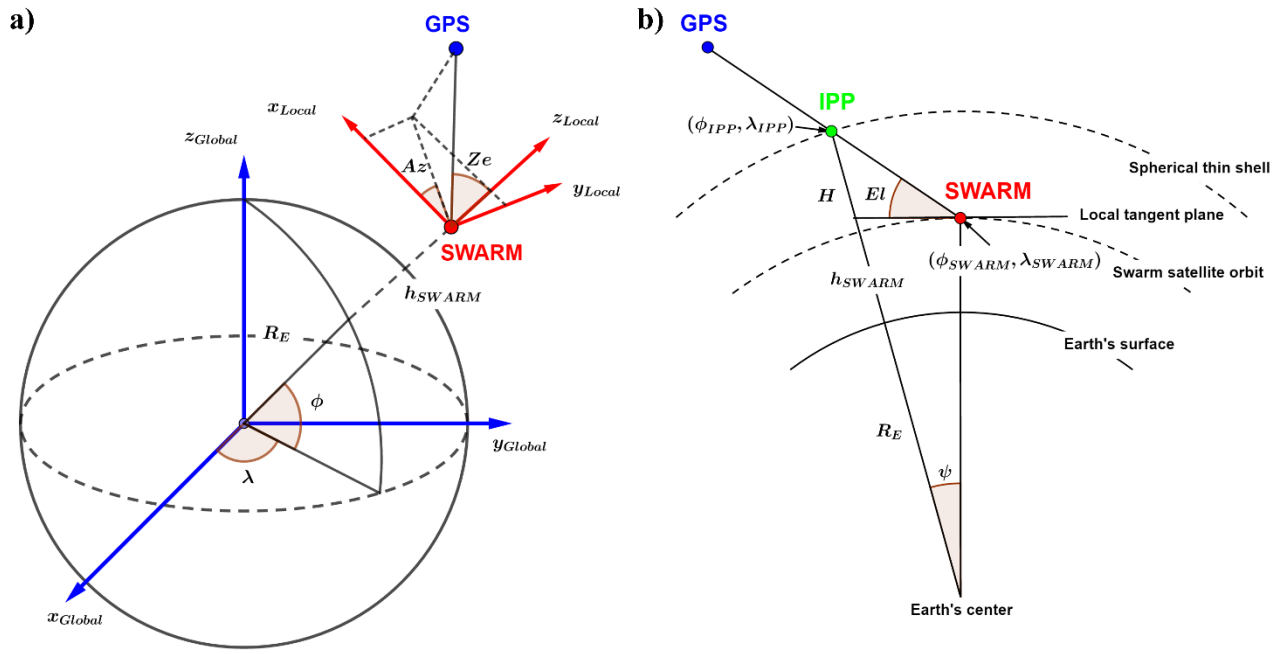

Figure 1: a) Global and Local Cartesian coordinate systems representation; b) Spherical thin shell approximation representation, orthogonal section along the Azimuth angle between Swarm and GPS satellites.

It is important to note that, because TEC is an integral quantity between LEO and GPS satellites, ROTI values cannot be associated either to Swarm or GPS positions. Here, we applied the customary methodology applied in the calculation of TEC values for ground-based GNSS receivers, i.e., the spherical thin shell approximation (Klobuchar, 1987). The spherical thin shell approximation geometric representation is given in the panel b) of Figure 1. Swarm is the receiver, whose local tangent plane is the one identified by the (x_{Local}, y_{Local}) plane, and the GPS position is given by the angles specified in (15). A spherical thin shell is placed at altitude H above Swarm (then at altitude h_{SWARM} + H to the Earth's surface). In TITIPy, H = 400 km. By following Klobuchar (1987) and Leick et al. (2015), the coordinates of the Ionospheric Pierce Point (IPP), i.e., the point where the link path between GPS and Swarm satellites pierces the spherical thin shell, can be deduced from spherical trigonometric relations and (15) (Figure 1):

$$\begin{cases} \psi = \dfrac{\pi}{2} - El - \arcsin\left(\dfrac{\mathrm{R_E} + h_{\mathrm{SWARM}}}{\mathrm{R_E} + h_{\mathrm{SWARM}} + \mathrm{H}} \cos El\right) \\ \varphi_{\mathrm{IPP}} = \arcsin\left(\sin\varphi_{\mathrm{SWARM}} \cos\psi + \cos\varphi_{\mathrm{SWARM}} \sin\psi \cos Az\right), \\ \lambda_{\mathrm{IPP}} = \lambda_{\mathrm{SWARM}} + \arcsin\left(\dfrac{\sin\psi \sin Az}{\cos\varphi_{\mathrm{IPP}}}\right) \end{cases} \quad (16)$$

where R_E is the Earth's radius, $(\lambda_{\mathrm{SWARM}}, \varphi_{\mathrm{SWARM}})$ are the geodetic longitude and latitude of Swarm satellite, ψ is the angle to the center of the Earth between Swarm and IPP, $(\lambda_{\mathrm{IPP}}, \varphi_{\mathrm{IPP}})$ are the geodetic longitude and latitude of the IPP. $(\lambda_{\mathrm{IPP}}, \varphi_{\mathrm{IPP}})$ are the coordinates to which calculated ROTI values are associated.

4. TITIPy design and workflow

TITIPy is a stand-alone Python tool composed by several scripts linked together. The flow chart depicting the TITIPy design and workflow is given in Figure 2. The description of each Python script composing TITIPy is the topic of this Section.

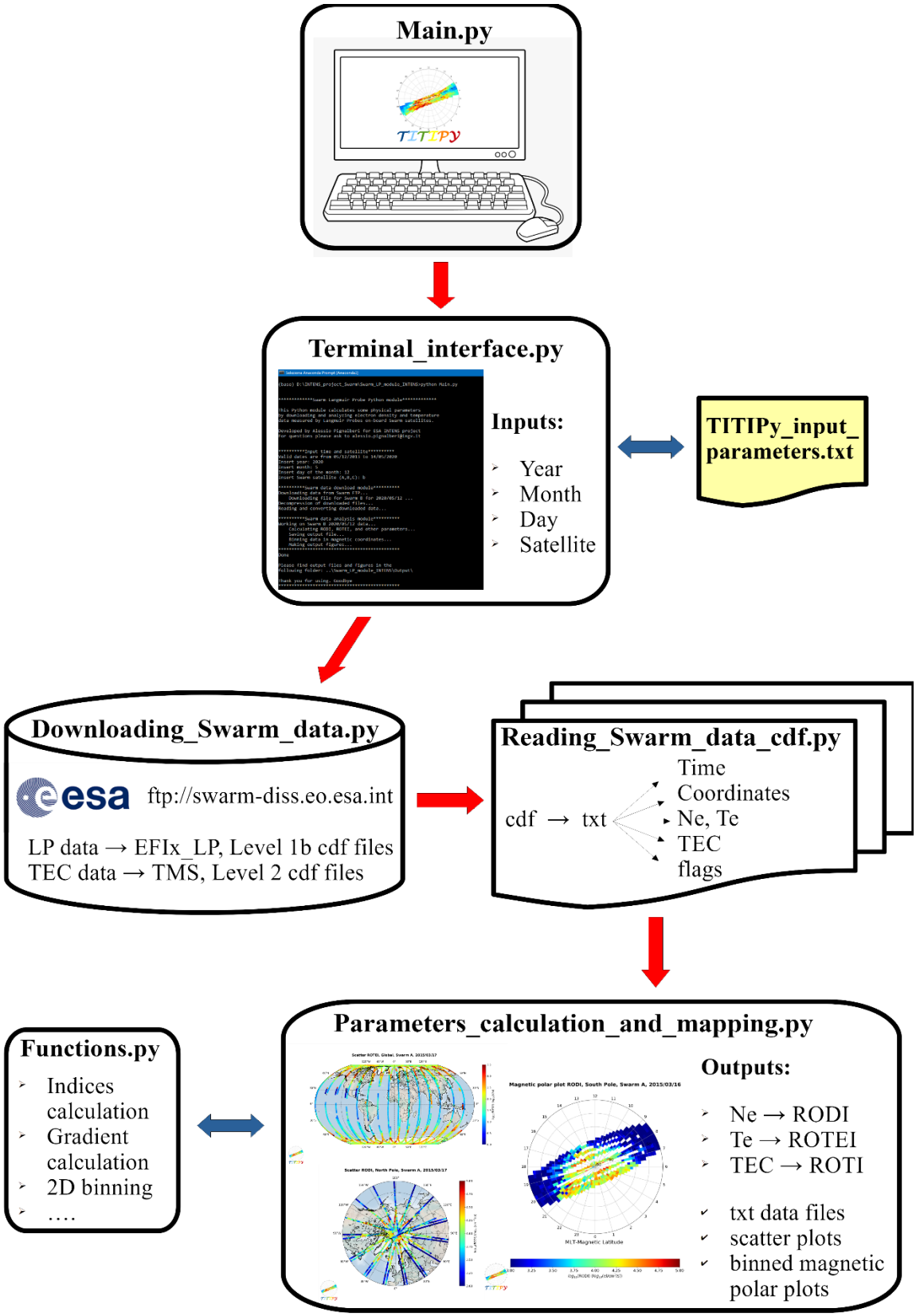

257

258 **Figure 2:** Flow chart representing TITIPy workflow and corresponding Python scripts.

259

260 **4.1 TITIPy launching and Python environment and dependencies**

TITIPy tool has been developed specifically for Linux-based operating systems and Python 3.7.6+ versions. It needs some not built-in Python libraries to run. All information on requirements, Python environment and needed dependencies are collected in the *README.md* file given along with TITIPy code. The *LICENSE* file is also given.

Main.py is the Python script to launch a TITIPy run. It imports and runs the other scripts of the tool, and controls the workflow. TITIPy can be run from terminal simply by navigating to the corresponding folder tool and by typing the following command:

```
python Main.py
```

Alternatively, any Python IDLE (Integrated Development and Learning Environment) can be used to run the script *Main.py*.

In the file *TITIPY_input_parameters.txt*, some run parameters, other than those defined through the terminal interface, can be defined.

Results of the TITIPy run, data and figures (if wanted), are put in the folder (created during the run) named *YYYYMMDDS*, where *YYYY* = year, *MM* = month, *DD* = day of the month, and *S* = Swarm satellite (A, B, or C), chosen through the terminal interface.

4.2 Terminal interface

The script *Terminal_interface.py* contains the terminal interface to allow the user to input TITIPy run's info. Specifically, it asks to insert the year, month, day, and Swarm satellite (A, B, or C). It is possible to run TITIPy from the 5th December 2013 (Swarm's beginning of the mission) to 6 days before today (due to latency in Swarm's TEC data dissemination). Moreover, *Terminal_interface.py* reads the *TITIPY_input_parameters.txt* file to get further info on the TITIPy run like: whether or not plotting the results, selecting the width of the sliding window used for indices calculation (in seconds), and which type of TEC data using in ROTI calculation.

4.3 Downloading and analysis of Swarm data

The script *Downloading_Swarm_data.py* downloads and decompresses LP and TEC files from ESA Swarm FTP (ftp://swarm-diss.eo.esa.int). Swarm Level 1b LP data are those in the folder *…/Level1b/Latest_baselines/EFIx_LP/* on ESA Swarm FTP; while Level 2 TEC data are in *…/Level2daily/Latest_baselines/TEC/TMS/*. Downloaded cdf files are put in the created folder *.../YYYYMMDDS/Downloaded_data/*.

The script *Reading_Swarm_data_cdf.py* reads the downloaded cdf files, calculates several quantities, and saves data in simple text files. Data are put in the created folder *.../YYYYMMDDS/Organized_data/*. In addition to information about time, location, physical quantities, and flags, the following quantities are here calculated:

- Universal Time: $UT = \left(3600 \cdot hour + 60 \cdot minute + second + 0.001 \cdot millisecond\right) / 3600$;
- Local Time: $LT = \left(UT + longitude / 15\right)\%24$, where % is the modulo operation;
- DOY (*Day Of the Year*): day from the beginning of the year;
- Height of the Swarm satellite: $h_{SWARM} = radius - R_E$, where *radius* is the distance of Swarm satellite from the Earth's center, and R_E is the Earth's radius (6371.007 km);
- Quasi-Dipole (QD) magnetic coordinates (Emmert et al., 2010; Laundal and Richmond, 2017): QD coordinates are calculated at the Swarm position for the specific *UT* hour;
- Magnetic Local Time (MLT) in QD coordinates.

4.4 Calculation and mapping of ionospheric indices

The script *Parameters_calculation_and_mapping.py* calculates the ionospheric indices (RODI, ROTEI, ROTI), for the selected day and Swarm satellite, by application of Section 3 formulas, and saves the results in the way of text files and figures (if wanted) in the created folder .../*YYYYMMDDS*/*Output/*. The script *Functions.py* contains several functions that are used for indices calculation and binning.

LP output file, named *Swarm_LP_S_YYYY_MM_DD_output.txt*, contains time, position, measured LP quantities, flags, calculated RODI (and related quantities defined in Section 3.1) and ROTEI (and related quantities defined in Section 3.2) time series at 2 Hz rate. TEC output files (32 files, one for each GPS satellite), named *Swarm_TEC_S_YYYY_MM_DD_PRNpp_output.txt* (where *pp* is the PRN of GPS satellite), contain time, position, measured TEC variables, and calculated ROTI (and related quantities defined in Section 3.3) time series at 1 Hz rate.

As said before, by default, the width of the sliding window used for indices calculation is set to 10 seconds (De Michelis et al., 2020) in order to catch small-scale fluctuations in measured data. However, this parameter can be changed in the *TITIPY_input_parameters.txt* to put the attention on different scales. Moreover, by default, absolute sTEC (slant total electron content) values are used for ROTI calculation. In the *TITIPY_input_parameters.txt*, the user can also decide to use absolute vTEC (vertical total electron content) or relative sTEC values for ROTI calculation.

TITIPy produces several output figures (if this option is not deactivated in *TITIPY_input_parameters.txt* file), in different formats and geographic projections, for calculated indices and measured quantities. A selection of these is shown in Figure 3 for the ROTEI index, for Swarm B, on the 25th August 2018, the main phase day of a geomagnetic storm (Piersanti et al., 2020). Two main types of figures are produced: scatter plots in geographic coordinates and binned polar plots in QD coordinates. Panels a), b), and c) represent scatter plots of ROTEI calculated values in a Global, North Pole, and South Pole view, respectively. Remember that ROTEI (the same for RODI) values are calculated in-situ at Swarm orbit position; while ROTI values are associated to the IPP position. Panels d) and e) of Figure 3 represent binned polar plots in QD coordinates of ROTEI for the North and South Magnetic Poles, respectively. The binning is done as a function of QD latitude (from ±40° to ±90° in steps of 2°) and MLT (from 0 to 24 in steps of 0.25, i.e., 15 minutes), and the median value of each bin is represented. Binned polar plots in QD coordinates are particularly suited to put in evidence the latitudinal distribution of fluctuations for the different local hours sounded by Swarm satellites. It is worth highlighting that Swarm satellites cover different MLT sectors during the mission lifetime. TITIPy produces also corresponding plots for the Swarm measured quantities *N*e, *T*e, and TEC.

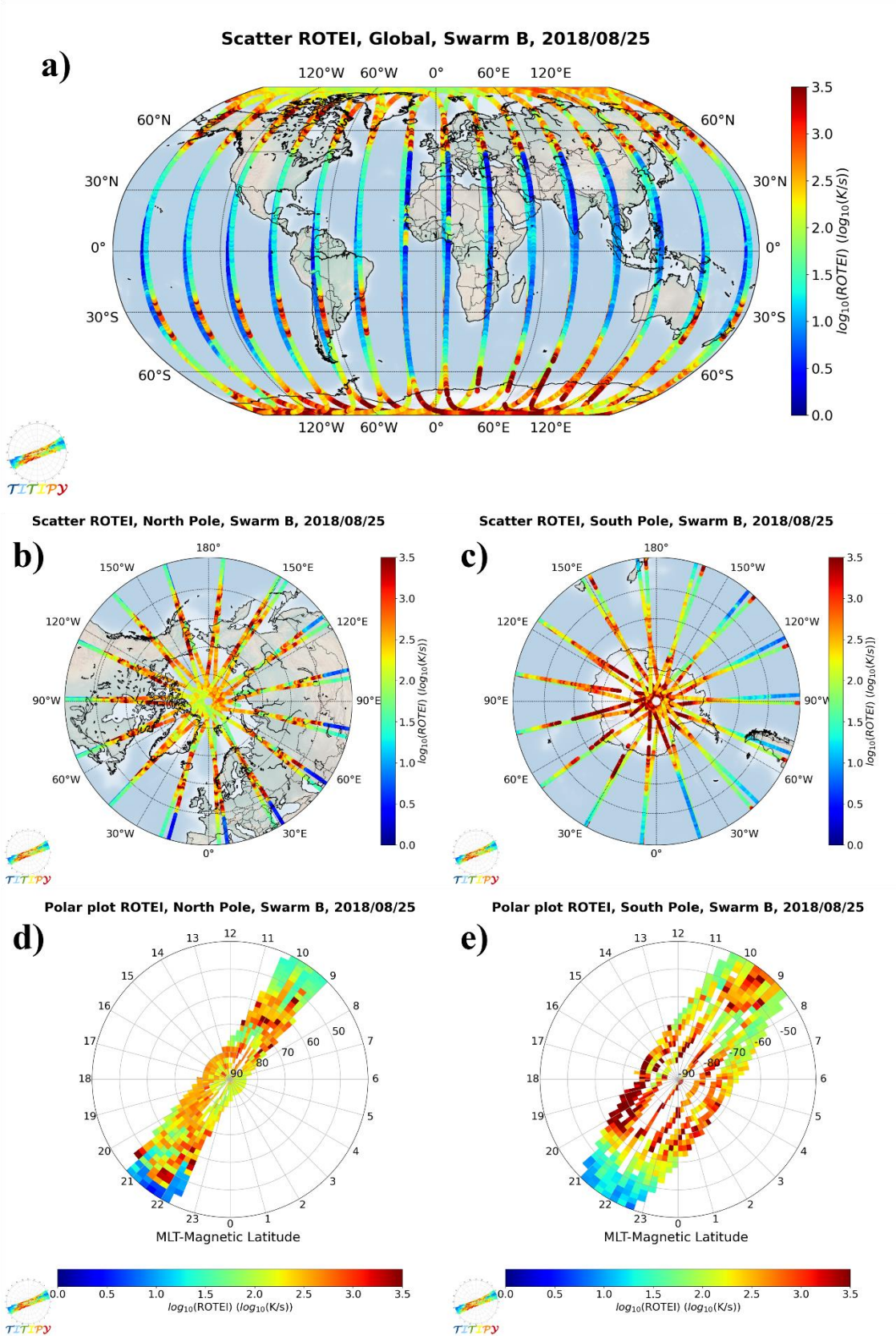

Figure 3: Examples of TITIPy output plots for the ROTEI index calculated through Swarm B data collected on 25 August 2018: a) Global scatter plot; b) North Pole scatter plot; c) South Pole scatter plot; d) Binned polar plot in QD magnetic coordinates for the North Magnetic Pole; e) Binned polar plot in QD magnetic coordinates for the South Magnetic Pole. The scale is the same across all plots.

5. Example of TITIPy application: the St. Patrick 2015 geomagnetic storm

One of the most fruitful usage of these ionospheric indices is the characterization of the topside ionosphere state during the development of a geomagnetic storm. In fact, geomagnetic storms can strongly impact on the physical and chemical state of the ionospheric plasma by producing fluctuations at very small spatial and temporal scales (Buonsanto, 1999; Prölss, 1995). This is why, it is here shown the application of TITIPy tool during some days encompassing the geomagnetic storm happened on 17 March 2015 (the so-called St. Patrick storm). It was the most intense geomagnetic storm of the solar cycle 24, classified as severe (Kamide and Kusano, 2015). Besides its intensity, the 2015 St. Patrick storm has been here selected because it is one of the most studied (Astafyeva et al., 2015), even through the application of these ionospheric indices (Cherniak et al., 2015; Cherniak and Zakharenkova, 2016; De Michelis et al., 2020).

Figures 4 and 5 show the trend of RODI, ROTEI, and ROTI indices during the different phases of the 2015 St. Patrick storm at high-magnetic latitudes, for both hemispheres. Specifically, binned polar plots in QD magnetic coordinates, for the Northern (Figure 4) and Southern (Figure 5) hemisphere, of RODI, ROTEI, and ROTI indices calculated through Swarm A data collected from 16 to 19 March 2015, are shown. The first day (16 March) is a quiet day before the storm commencement; the main phase of the storm happened during the course of 17 March, with a recovery phase extending for several days after. ROTI values in Figures 4 and 5 are those calculated by joining all 32 GPS satellites. Compared to RODI and ROTEI, ROTI calculated values cover a wider region due to the fact that they are referred to the IPP coordinates (16); then, depending on the specific GPS Azimuth and Elevation angles, positions different from the Swarm orbit are covered.

It is evident how ionospheric indices change in intensity and location during the course of the storm. For example, ROTI values increase during the main phase of the storm (17 March) in the polar cap extending also to auroral and sub-auroral latitudes in the successive recovery phase days (albeit with a decreasing intensity). ROTEI values also manifest an increase in their intensity passing from quiet to disturbed conditions, but what it is more interesting is the expansion of the region covered by those disturbances under disturbed conditions. In fact, while under quiet conditions (16 March) high ROTEI values are visible only at very high latitudes, during disturbed conditions (17 to 19 March) the region characterized by high ROTEI values enlarges by including also sub-auroral latitudes. A similar, albeit less evident, behavior is also exhibited by RODI values which, in a first stage, grow in intensity and expand towards lower latitudes (17 March), then they decrease in intensity during 18 March to rise again during 19 March. This behavior is particularly evident for Northern latitudes (Figure 4) and is associated to the different *phases* of the storm. In fact, RODI being derived from in-situ electron density values is affected by *positive* and *negative* phases of the storm (Prölss, 1995), causing increasing or decreasing in the topside electron density. In particular, 18 March is a negative phase day of the storm and the lowering of the background electron density seems to damp possible irregularities. This is also experienced by ROTI but with a less extension due to the integral nature of ROTI values.

Magnetic polar plots, like those shown in Figure 4 and 5, can be of great value for ionospheric studies and to link the behavior exhibited by these ionospheric indices to possible source mechanisms which are typical of high latitudes like electric currents, plasma transport, particle precipitation, and thermospheric heating.

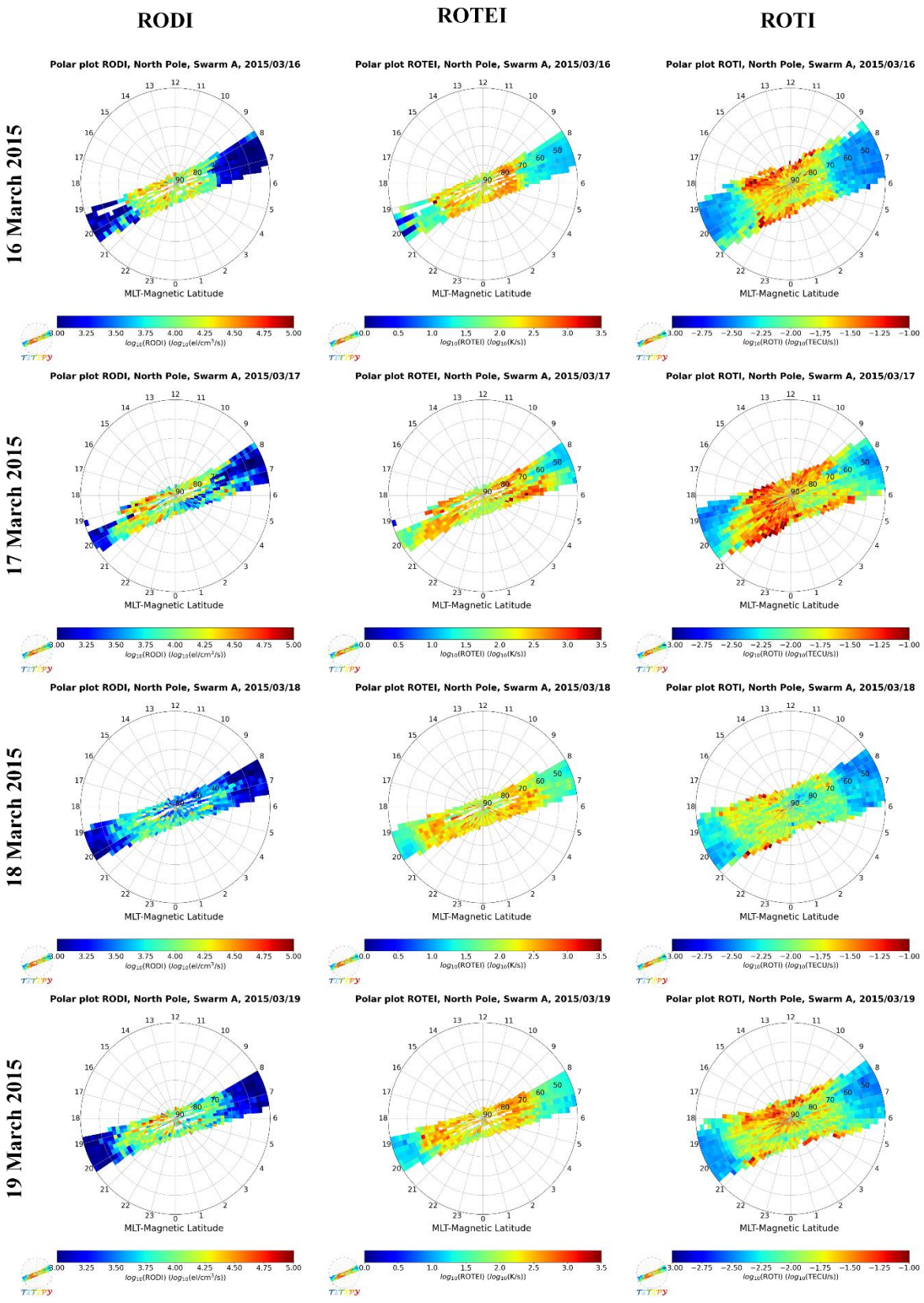

Figure 4: Binned polar plots in QD magnetic coordinates for the North Magnetic Pole for RODI (left panels), ROTEI (middle panels), and ROTI (right panels) indices calculated through Swarm A data collected from 16 to 19 March 2015 (from top to bottom). Scales, for each index, are the same across all plots.

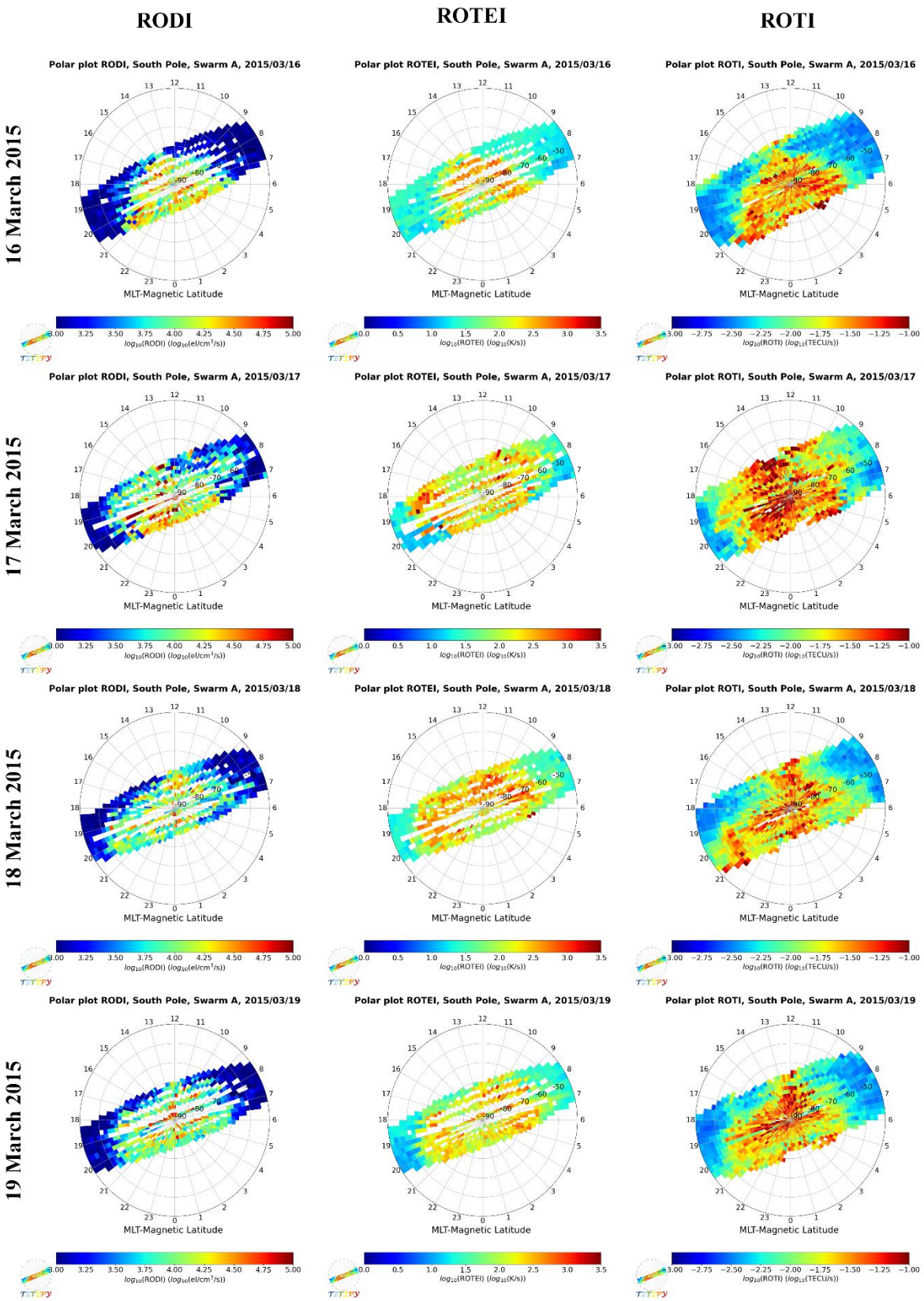

Figure 5: Same as Figure 4 but for the South Magnetic Pole.

6. Conclusions

TITIPy is a Python tool specifically developed for the calculation and mapping of topside ionosphere turbulence indices that can be derived through ESA Swarm satellites mission measurements. The tool allows for obtaining the well-known RODI and ROTI indices through the analysis of electron density measurements from Langmuir Probes and from TEC derived values, respectively. Moreover, by applying the same methodology used for RODI calculation, the new index ROTEI has been defined based on electron temperature measurements by Langmuir Probes. RODI and ROTEI describe fluctuations and irregularities at small spatial and temporal scales in the in-situ topside electron density and temperature. In contrast, ROTI values are connected to non-local irregularities embedded in the integral of the electron density encompassing the topside ionosphere and the plasmasphere. The spherical thin shell geometric approximation has been here applied for the localization of ROTI values along the link path between LEO Swarm and GPS satellites. The study of these indices allows to characterize the turbulent state of the topside ionosphere and to link their spatial and temporal variability to physical mechanisms involved in plasma electrodynamics. TITIPy is open-source and freely downloadable at https://github.com/pignalberi/TITIPy.

Acknowledgements

This research is partially supported by the Italian MIUR-PRIN grant 2017APKP7T on Circumterrestrial Environment: Impact of Sun-Earth Interaction.

Thanks to the INTENS (*Characterization of IoNospheric TurbulENce level by Swarm constellation*) team people (http://intens.rm.ingv.it/) for their support, stimulating discussions, and important advices in the development and testing of the software.

Thanks to the European Space Agency for making Swarm data publicly available via ftp://swarmdiss.eo.esa.int, and for the considerable efforts made for the Langmuir probes and POD antennas data calibration and maintaining.

Code availability

- Code name: TITIPy
- Developer: Alessio Pignalberi
- Email: alessio.pignalberi@ingv.it
- Contact address: Istituto Nazionale di Geofisica e Vulcanologia, Via di Vigna Murata, 605, 00143, Rome, Italy
- First release: July 2020

TITIPy (*Topside Ionosphere Turbulence Indices with Python*) is a stand-alone Python tool developed for the calculation and mapping of RODI, ROTI, and ROTEI indices, for the characterization of the turbulent state of the topside ionosphere. TITIPy is open-source and freely downloadable at https://github.com/pignalberi/TITIPy. TITIPy code is licensed under CC BY-NC-SA 3.0 (Creative Commons Attribution-NonCommercial-ShareAlike 3.0 Unported License, http://creativecommons.org/licenses/by-nc-sa/3.0/). TITIPy was developed in Python language (v3.7.6) under Linux Ubuntu (20.04 LTS) operating system. All information on requirements, Python environment and needed dependencies are provided in the *README.md* file.

Authorship Statement

Alessio Pignalberi has conceived, developed, implemented, and tested the TITIPy Python code. Moreover, he has written the manuscript and is the responsible for the dissemination and maintaining of the code.

References

Astafyeva, E., Zakharenkova, I., and Forster, M., "Ionospheric response to the 2015 St. Patrick's day storm: A global multi-instrumental overview", *Journal of Geophysical Research: Space Physics*, 120, 9023-9037, doi:10.1002/2015JA021629, 2015. *Other than data*

Buchert, S., Zangerl, F., Sust, M., Andre, M., Eriksson, A., Wahlund, J. E., and Opgenoorth, H., "Swarm observations of equatorial electron densities and topside GPS track losses". *Geophysical Research Letters*, 42, 2088– 2092. https://doi.org/10.1002/2015GL063121, 2015.

Buonsanto, M. J., "Ionospheric storms-a review". *Space Science Reviews*, *88*(3/4), 563–601. https://doi.org/10.1023/A:1005107532631, 1999.

Cherniak, I., Krankowski, A., and Zakharenkova, I., "Observation of the ionospheric irregularities over the Northern Hemisphere: Methodology and service", *Radio Science*, 49, 653– 662, doi:10.1002/2014RS005433, 2014.

Cherniak, I., Zakharenkova, I., and Redmon, R. J., " Dynamics of the high-latitude ionospheric irregularities during the 17 March 2015 St. Patrick's Day storm: Ground-based GPS measurements", *Space Weather*, 13, 585– 597, doi:10.1002/2015SW001237, 2015.

Cherniak, I., and Zakharenkova, I., "High-latitude ionospheric irregularities: differences between ground- and space-based GPS measurements during the 2015 St. Patrick's Day storm". *Earth Planet Space*, 68, 136, https://doi.org/10.1186/s40623-016-0506-1, 2016.

De Michelis, P., Pignalberi, A., Consolini, G., Coco, I., Tozzi, R., Pezzopane, M., Giannattasio, F., and Balasis, G., "On the 2015 St. Patrick Storm Turbulent State of the Ionosphere: Hints from the Swarm Mission". *Journal of Geophysical Research: Space Physics*, 125, e2020JA027934, https://doi.org/10.1029/2020JA027934, 2020.

Emmert, J.T., Richmond, A.D., and Drob, D.P., "A computationally compact representation of Magnetic-Apex and Quasi-Dipole coordinates with smooth base vectors". *Journal of Geophysical Research: Space Physics*, doi:10.1029/2010JA015326, 2010.

Friis-Christensen, E., Lühr, H. and Hulot, G., "Swarm: A constellation to study the Earth's magnetic field". *Earth, Planets Space*, 58, 351–358. https://doi.org/10.1186/BF03351933, 2006.

Jin, Y., Spicher, A., Xiong, C., Clausen, L. B. N., Kervalishvili, G., Stolle, C., and Miloch, W. J., "Ionospheric plasma irregularities characterized by the Swarm satellites: Statistics at high latitudes". *Journal of Geophysical Research: Space Physics*, 124, 1262– 1282. https://doi.org/10.1029/2018JA026063, 2019.

Kamide, Y., and Kusano, K., "No major solar flares but the largest geomagnetic storm in the present solar cycle". *Space Weather*, 13:365–367, doi:10.1002/2015SW001213, 2015.

Kelley, M.C., "The Earth's Ionosphere". *International Geophysics (Book 96), Academic Press, 2 edition*, San Diego, USA, 2009.

Klobuchar, J. A., "Ionospheric Time-Delay Algorithm for Single-Frequency GPS Users". *IEEE Transactions on Aerospace and Electronic Systems*, vol. AES-23, 3, 325-331, doi: 10.1109/TAES.1987.310829, 1987.

463 Knudsen, D. J., Burchill, J. K., Buchert, S. C., Eriksson, A. I., Gill, R., Wahlund, J.-E., Åhlen, L., Smith, M.,
464 and Moffat, B., "Thermal ion imagers and Langmuir probes in the Swarm electric field instruments". *Journal*
465 *of Geophysical Research: Space Physics*, 122, 2655–2673. https://doi.org/10.1002/2016JA022571, 2017.

466 Laundal, K. M., and Richmond, A. D., "Magnetic Coordinate Systems". *Space Science Reviews*, 206, 27.
467 https://doi.org/10.1007/s11214-016-0275-y, 2017.

468 Leick, A., Rapoport, L., and Tatarnikov, D., "GPS Satellite Surveying. Fourth edition.", *John Wiley & Sons*,
469 doi:10.1002/9781119018612, 2015.

470 Lomidze, L., Knudsen, D. J., Burchill, J., Kouznetsov, A. and Buchert, S. C., "Calibration and validation of
471 Swarm plasma densities and electron temperatures using ground-based radars and satellite radio occultation
472 measurements". *Radio Science*, 53, 15–36, https://doi.org/10.1002/2017RS006415, 2018.

473 Moldwin, M., "An introduction to space weather*"*. *Cambridge: Cambridge University Press*.
474 https://doi.org/10.1017/CBO9780511801365, 2008.

475 Noja, M., Stolle, C., Park, J., and Luhr, H., "Long-term analysis of ionospheric polar patches based on CHAMP
476 TEC data". *Radio Science*, 48, 289– 301. https://doi.org/10.1002/rds.20033, 2013.

477 Pi, X., Mannucci, A.J., Lindqwister, U.J., and Ho, C.M., "Monitoring of global ionospheric irregularities using
478 the worldwide GPS network". *Geophysical Research Letters*, 24:2283, https://doi.org/10.1029/97GL02273,
479 1997.

480 Piersanti, M., De Michelis, P., Del Moro, D., Tozzi, R., Pezzopane, M., Consolini, G., Marcucci, M. F.,
481 Laurenza, M., Di Matteo, S., Pignalberi, A., Quattrociocchi, V., Diego, P.," From the Sun to Earth: effects of
482 the 25 August 2018 geomagnetic storm", *Annales Geophysicae*, 38(3), 703-724, doi:10.5194/angeo-38-703-
483 2020, 2020.

484 Prölss, G., "Ionospheric F-region storms", in *Handbook of Atmospheric Electrodynamics*, vol. 2, edited by H.
485 Volland, pp. 195–248, CRC Press, Boca Raton, Fla, 1995.

486 Ratcliffe, J.A., "An introduction to the ionosphere and magnetosphere". *Cambridge University Press*, 1972.

487 Rishbeth, H., and Garriott, O., "Introduction to ionospheric physics". *Academic press, New York*, International
488 geophysics series v. 14, 1969.

489 Stolle, C., Floberghagen, R., Luhr, H., Maus, S., Knudsen, D. J., Alken, P., Doornbos, E., Hamilton, B.,
490 Thomson, A. W. P., and Visser, P. N., "Space weather opportunities from the Swarm mission including near
491 real time applications". *Earth, Planets and Space*, 65(11), 1375– 1383.
492 https://doi.org/10.5047/eps.2013.10.002, 2013.

493 Swarm L1b Product Definition,
494 https://earth.esa.int/documents/10174/1514862/Swarm_L1b_Product_Definition, 2018.

495 Swarm L2 TEC Product Description, https://earth.esa.int/documents/10174/1514862/Swarm_Level-
496 2_TEC_Product_Description, 2017.

497 Tsunoda, R. T., "High-latitude *F* -region irregularities: A review and synthesis". *Reviews of Geophysics*, 26(4),
498 719– 760. https://doi.org/10.1029/RG026i004p00719, 1988.

499 van den IJssel, J., Forte, B. and Montenbruck, O., "Impact of Swarm GPS receiver updates on POD
500 performance". *Earth, Planets and Space*, 68**,** 85, https://doi.org/10.1186/s40623-016-0459-4, 2016.

501 Xiong, C., Stolle, C., and Lühr, H., "The Swarm satellite loss of GPS signal and its relation to ionospheric
502 plasma irregularities". *Space Weather*, 14, 563– 577. https://doi.org/10.1002/2016SW001439, 2016.

503 Xu, G., and Xu, Y., "GPS. Theory, Algorithms and Applications", *Springer-Verlag Berlin Heidelberg*,
504 doi:10.1007/978-3-662-50367-6, 2016.

505 Zakharenkova I., and Astafyeva E., "Topside ionospheric irregularities as seen from multisatellite
506 observations". *Journal of Geophysical Research: Space Physics*, 120(1), 807–824.
507 doi:10.1002/2014JA020330, 2015.

508 Zakharenkova, I., Astafyeva, E., and Cherniak, I.," GPS and in situ Swarm observations of the equatorial
509 plasma density irregularities in the topside ionosphere". *Earth, Planets and Space*, 68(1).
510 https://doi.org/10.1186/s40623-016-0490-5, 2016.